

②

DTIC ELECTE
JUN 03 1988

ITEM 19-ABSTRACT CONTINUED

(d₃₁ 0.03d₃₃) which would tend to minimize the couplings due to slight structural asymmetries. These resonances were also excited in this material.

| | |
|--------------------|-------------------------------------|
| Accession For | |
| NEIS OR&I | <input checked="" type="checkbox"/> |
| DDIC TAB | <input type="checkbox"/> |
| Unannounced | <input type="checkbox"/> |
| Justification | |
| By | |
| Distribution/ | |
| Availability Codes | |
| Avail and/or | |
| Dist | Special |
| A-1 | 20 |



Electrical excitation of flexural mechanical resonances in symmetrically electroded piezoelectric and ferroelectric specimens

Joseph E. Blue

Naval Research Laboratory, Underwater Sound Reference Detachment, P. O. Box 568337, Orlando, Florida 32856-8337

Peter J. Chen

Sandia National Laboratories, Albuquerque, New Mexico 87185

Theodore A. Henriquez and Robert Y. Ting

Naval Research Laboratory, Underwater Sound Reference Detachment, P. O. Box 568337, Orlando, Florida 32856-8337

(Received 21 November 1986; accepted for publication 22 December 1987)

A clear understanding of the relationship of mechanical and acoustical excitation to electrical output of piezoelectric materials is important in the design of large-area acoustic sensors. Chen [Il Nuovo Cimento 2 D, 1145-1155 (1983)] has reported on electrical excitation of flexural mechanical resonances that are not accompanied by detectable electrical disturbances in the ac drive circuits in a number of different specimens such as X- and Z-cut quartz, Z-cut LiNbO_3 , ADP, PZTs, BaTiO_3 , and PLZTs. These observations have raised questions about the understanding of electromechanical interactions. Speculations about the cause of the resonances include the possibility of incompleteness of the constitutive equations of piezoelectricity, surface polarization phenomena, and simple couplings due to slight structural asymmetries. In the latter regard, the objective was to see if the flexural resonances could be easily excited in a Ca-doped PbTiO_3 disk having a very small lateral piezoelectric constant ($d_{31} \approx 0.03d_{33}$) which would tend to minimize the couplings due to slight structural asymmetries. These resonances were also excited in this material.

PACS numbers: 43.88.Ar, 43.88.Fx, 43.20.Ks

INTRODUCTION

A clear understanding of the relationship of mechanical and acoustical excitation to electrical output is fundamental to the design of large-area acoustic sensors for improving the signal-to-noise ratio in the presence of turbulent flow. Chen's¹⁻⁶ observations of electrically excited mechanical resonances in a number of piezoelectric and ferroelectric disk specimens raise questions about the completeness of our understanding.

Simultaneous announcements^{1,2} have recently been made concerning the existence of electrically excitable mechanical resonances in piezoelectric and virgin ferroelectric specimens for which the ac drive circuits do not exhibit any detectable electrical disturbance on a normal immittance plot. This observation is valid even with the use of a very sensitive capacitor-bridge circuit due to A. G. Beattie of Sandia National Laboratories and R. N. Thurston of Bell Communications Research. Examples of some of the piezoelectric specimens that have been examined are X- and Z-cut quartz and ADP, while those of ferroelectric specimens include slim loop ferroelectrics, Z-cut LiNbO_3 , PZT65/35, PLZT7/65/35, BaTiO_3 ceramic, Clevite PZT8, and Channel 5500 ceramic.

Since the original announcements, much effort has been devoted to the quantitative characterization of the resonance modes of virgin PLZT7/65/35 and PZT65/35 disk speci-

mens.^{3,4} The resonance modes exhibited by the specimens are flexural. The resonance frequencies and the quadrature components of the axial displacements with respect to the driving voltages correspond to the natural frequencies and modes predictable by the classical bending theory of thin elastic plates,⁷ and the in-phase components of the displacements are not always zero during the occurrences of these resonances. Therefore, the resultant amplitudes of the displacements yield contour patterns that cannot be discerned by dust pattern and holographic techniques as to the nature of the resonance modes, except in particular cases.

Perhaps the most important experimental result is that reported in Ref. 5. It is shown that a disk of virgin PLZT7/65/35 in traction-free condition displaces "parabolically" along any diameter upon the application of a small axial dc voltage and that the displacements are in the positive direction of the electric field. This is a purely flexural phenomenon and is not accompanied by detectable changes in specimen thickness as predicted by the classical notions of piezoelectricity and electrostriction. This phenomenon has been subsequently detected in other ferroelectric ceramics and is a manifestation of a new coupling mechanism that gives rise to the flexural resonant modes mentioned earlier.⁸

In this article, we present experimental results which show the existence of electrically driven flexural resonance modes in a disk specimen of Ca-doped PbTiO_3 ceramic. This ceramic has the trade name C-26 and was prepared by To-

shiba Ceramics Co., Ltd. When poled, this ceramic has very unusual piezoelectric properties, viz., the piezoelectric constant $d_{33} = 62.8 \times 10^{-12}$ m/V and the piezoelectric constant d_{31} is nearly zero. The latter has been estimated to be approximately 3% of d_{33} . This means that there is very little cross coupling upon the application of an electric field in the direction of remanent polarization, and it would be very difficult to excite flexural resonance modes via standard methods of using nonsymmetrical electrode patterns on the major surfaces of a disk. The major surfaces of the disk that we have examined were fully electroded, and the disk was driven via the application of ac voltages between the electrodes. The results of the flexural resonance modes that we have obtained are completely consistent with those that we have obtained for other compositions. In addition, since the disk has been poled, a conventional "thickness" resonance was also detected. This thickness resonance is, of course, accompanied by easily detectable electrical disturbances in the ac drive circuit.

I. EXPERIMENTAL DETAILS

The displacements of the surfaces of a disk are measured by means of a dual beam laser interferometer developed at Sandia National Laboratories. This interferometer is actually two modified displacement interferometers with a single He-Ne light source. Each of the interferometers has a quadrature leg so that the direction of motion can also be determined. The signal beams of the interferometers are perpendicularly directed at the opposite surfaces of the specimen. Careful alignment of the signal beams ensures that we can indeed measure the displacements of opposite points of the major surfaces. Rotation and translation of the specimen with respect to the signal beams thus permit us to determine its vibrational mode shapes.

The Ca-doped PbTiO_3 disk specimen under consideration has a diameter of 2.494×10^{-2} m and a thickness of 1.51×10^{-3} m. The latter dimension includes the fired-on silver electrodes whose thicknesses are not known. Since the specimen was not polished and the silver electrodes were not spectral reflectors, very small mirrors were glued at the centers of the major surfaces and on the positive surface separated by 143° at a radius of 1.119×10^{-2} m. Specific data were collected at these mirror locations as it was not possible to scan the major surfaces. There is, however, no difficulty in identifying the resonance modes. During the course of the measurements, the specimen was gently held at its edge in the vertical plane by three symmetrically located small sponges within a rather massive brass annulus. The aluminum base on which the annulus rests may be translated.

Electrical contact with the specimen was effected with the use of fine gold wires attached to the electroded regions with drops of silver paint. The specimen was also connected in series with an integrating capacitor whose capacitance is large compared to that of the specimen. This permits the determination of the electrical charge.

During the course of an experiment, we measure the voltage corresponding to the amplitude of a full interference fringe, the voltage corresponding to the interference fringe due to the displacement of a surface point, and the phase

angle between the fringe voltage of the displacement and the applied voltage. We also measure the amplitude of the voltage across the integrating capacitor, and the phase angle between this voltage and the applied voltage.

Since each degree of the interference fringe corresponds to 8.7889×10^{-10} m, the amplitude u_0 of the displacement of a surface point is given by

$$u_0 = \sin^{-1}(V_m/V_f) 8.7889 \times 10^{-10} \text{ m},$$

where V_m is the fringe voltage amplitude of the displacement and V_f is the fringe voltage amplitude of a full interference fringe. This formula is valid when the fringe voltage amplitude of the displacement is less than that of a full interference fringe. Repeatable results of the order of 10^{-12} m can be obtained with this system.

The amplitude Q_0 of the charge Q on the integrating capacitor is given by

$$Q_0 = CV_{C0},$$

where C is its capacitance, and V_{C0} is the amplitude of the voltage across it. The current I in the circuit is given by Q .

The applied alternating voltage V may be represented by

$$V = V_0 \sin \omega t,$$

where V_0 is its amplitude, ω is its frequency, and t is the time. It is convenient to reference the voltage with respect to the surface at which the remanent polarization is directed such that, when ωt is in the neighborhoods of $2n\pi$, $n = 0, 1, 2$, the polarity of the surface switches from $-$ to $+$. This surface shall be designated as the $-$ surface and all quantities associated with it shall be denoted with the subscript $-$. The opposite surface shall be designated as the $+$ surface and all quantities associated with it shall be denoted with the subscript $+$. The mechanical displacements u_{\pm} are, therefore,

$$u_{\pm} = u_{0\pm} \sin(\omega t + \phi_{\pm}),$$

where $u_{0\pm}$ are their amplitudes and ϕ_{\pm} are the phase angles between the displacements and the driving voltage.

Let u_f denote the flexural mechanical displacement due to the new electromechanical coupling phenomenon. It may be expressed in the form

$$u_f = u_{f0} \sin(\omega t + \phi_f),$$

where u_{f0} is its amplitude and ϕ_f its phase angle with respect to the driving voltage. Let u_p denote the mechanical displacements due to conventional piezoelectric coupling. They are of the form

$$u_{p\pm} = u_{p0} \sin(\omega t + \phi_{p\pm}),$$

where u_{p0} is their amplitude and $\phi_{p\pm}$ are their phase angles with respect to the driving voltage. Clearly, we must have

$$\phi_{p-} = \phi_{p+} \pm \pi.$$

Therefore,

$$u_{p-} = -u_{p+} = -u_{p0} \sin(\omega t + \phi_{p+}).$$

Given the preceding results, we see that

$$u_{+} = u_f + u_{p+}, \quad u_{-} = u_f + u_{p-},$$

and upon equating the amplitudes of their in-phase and quadrature components, we obtain, respectively, for the $+$ surface

$$u_{0+} \cos \phi_+ = u_{f0} \cos \phi_f + u_{p0} \cos \phi_{p+},$$

$$u_{0+} \sin \phi_+ = u_{f0} \sin \phi_f + u_{p0} \sin \phi_{p+},$$

and, respectively, for the $-$ surface

$$u_{0-} \cos \phi_- = u_{f0} \cos \phi_f - u_{p0} \cos \phi_{p+},$$

$$u_{0-} \sin \phi_- = u_{f0} \sin \phi_f - u_{p0} \sin \phi_{p+}.$$

The sums of the amplitudes of the in-phase and quadrature components of the $+$ and $-$ surfaces, therefore, give twice the amplitudes of the in-phase and quadrature components of the flexural mechanical displacements due to the new electromechanical coupling phenomenon, viz.,

$$u_{0+} \cos \phi_+ + u_{0-} \cos \phi_- = 2u_{f0} \cos \phi_f,$$

$$u_{0+} \sin \phi_+ + u_{0-} \sin \phi_- = 2u_{f0} \sin \phi_f.$$

On the other hand, the difference between the amplitudes of the in-phase and quadrature components of the $+$ and $-$ surfaces give twice the amplitudes of the in-phase and quadrature components of the mechanical displacements due to conventional piezoelectric coupling. They are

$$u_{0+} \cos \phi_+ - u_{0-} \cos \phi_- = 2u_{p0} \cos \phi_{p+},$$

$$u_{0+} \sin \phi_+ - u_{0-} \sin \phi_- = 2u_{p0} \sin \phi_{p+}.$$

Experimentally, we may measure the amplitudes of the in-phase and quadrature components of the mechanical displacements of as many selected opposite surface points of the $+$ and $-$ surfaces as desired. It is, therefore, a simple matter to resolve the measured results into the flexural displacements due to the new coupling phenomenon and the displacements due to conventional piezoelectric coupling.

In a similar vein, the charge is given by

$$Q = Q_0 \sin(\omega t + \phi_Q),$$

where ϕ_Q is the phase angle between the charge and the driving voltage. Therefore, the in-phase component of Q is $Q_0 \sin \omega t \cos \phi_Q$, and the quadrature component of Q is $Q_0 \cos \omega t \sin \phi_Q$.

The onset of a flexural mechanical resonance is taken to be that frequency at which the amplitude of the quadrature component of the flexural displacement, $u_{f0} \sin \phi_f$, has relative maximum magnitude for each pair of opposite surface points of the $+$ and $-$ surfaces. The corresponding amplitude of the in-phase components, $u_{f0} \cos \phi_f$, at that frequency are not, in general, zero. On the other hand, an electrical resonance at a particular frequency is said to exist if

$$\phi_Q = n\pi/2, \quad n = 1, 3, 5, \dots$$

II. EXPERIMENTAL RESULTS

The preceding analysis illustrates how we may resolve the measured displacements of pairs of opposite surface points into the flexural and thickness components due, respectively, to the new electromechanical coupling phenomenon and conventional piezoelectric coupling. If the data of the displacements are available for a sufficient number of opposite surface points, the vibrational patterns due to the two mechanisms can be determined.

For the Ca-doped PbTiO_3 specimen under consideration, data may only be collected at the four mirror locations, viz., at the centers of the major surfaces of the disk and

at the same radial location on the $+$ surface separated by 143° . Therefore, the results that we present in this article serve to illustrate the existence of the flexural resonances and the single thickness resonance that we have mentioned earlier.

Up to a driving voltage frequency of 120 kHz, three resonances were detected at the center mirrors. They occur at 16.7, 68.6, and 112.16 kHz. The first two are, respectively, the flexural resonance modes with 1 nodal ring and 2 nodal rings; the third at 112.16 kHz is the standard thickness resonance due to conventional piezoelectric coupling. The latter thickness resonance is accompanied by easily detectable electrical disturbance in the ac drive circuit. In Fig. 1, we give the amplitudes of the in-phase component of the charge, $Q_0 \cos \phi_Q$, and the quadrature component of the charge, $Q_0 \sin \phi_Q$, over the frequency range 110–115 kHz. The vibrational pattern of this resonance for disk specimen of PZT65/35 composition is given in Ref. 6, where the results indicate that the pattern is not one dimensional with large thickness changes at the center and decaying monotonically towards the edge.

In order to facilitate the ease of presentation of the subsequent results, we let the pair (m, n) denote the flexural resonance mode with m nodal diameters and n nodal rings.

In Figs. 2 and 3, we give the amplitudes of the in-phase component, $u_{0-} \cos \phi_-$, and the quadrature component, $u_{0-} \sin \phi_-$, of the resonance modes (0,1) and (0,2) at the center of the disk, respectively, as functions of frequency. Similar results were obtained for the $+$ surface. Resonances occur when $u_{0-} \sin \phi_-$ have maximum magnitudes. In Figs. 4 and 5, we exhibit the plots of $u_{0-} \sin \phi_-$ as functions of the amplitude of the driving voltage of the (0,1) and (0,2) modes, respectively. Notice that the results are very linear.

In order to ascertain the existence of other flexural resonance modes, experimental data were collected at the two radial locations on the $+$ surface separated by 143° . The radius of the two locations is 1.119×10^{-2} m. In Figs. 6 and 7, we give the amplitudes of the quadrature component $u_{0+} \sin \phi_+$ as a function of frequency from 1–120 kHz. Ten additional resonances were detected in this frequency range. By comparing the results of Figs. 6 and 7 as to the signs of

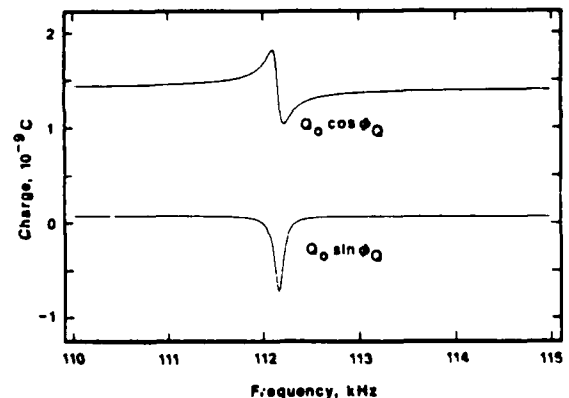


FIG. 1. Amplitudes of the in-phase and quadrature components of the charge versus frequency. Amplitude of the driving voltage is 2.5 V.

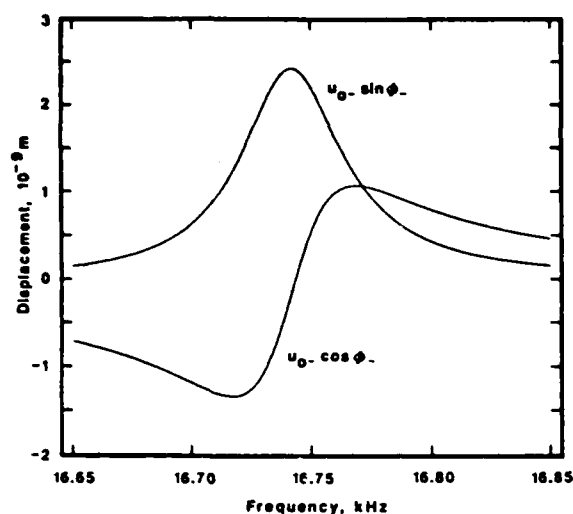


FIG. 2. Amplitudes of the in-phase, $u_{0+} \cos \phi_+$, and quadrature, $u_{0-} \sin \phi_-$, components of the (0,1) mode at the center of the — surface versus frequency. Amplitudes of the driving voltage are 2.5 V.

$u_{0+} \sin \phi_+$ and the frequencies of the resonances with the natural frequencies of a thin disk with free edge (see, e.g., Cowell and Hardy¹⁰), the ten additional resonances can be identified. The results are given in Table I.

It is of importance to note that the number of resonances is as predicted by the classical bending theory of thin plates, no more and no less. Therefore, the forcing induced by the electric field must have all the characteristics of the natural modes. The theory proposed in Ref. 9 has this property.

It is of interest to note that the (7,0) mode which occurs at 110.8 kHz is not accompanied by any detectable electrical disturbance in the drive circuit, as indicated by the data of Fig. 1. This is also true for all the other flexural resonance modes.

Notice that the amplitudes of the quadrature component, $u_{0+} \sin \phi_+$, of the conventional thickness resonance at 112.16 kHz are not equal at the two radial locations separated by 143°. This is because a complicated flexural vibrational pattern is superimposed on the thickness resonance. This observation is based on the results given in Ref. 6 concerning a disk of PZT65/35 composition.

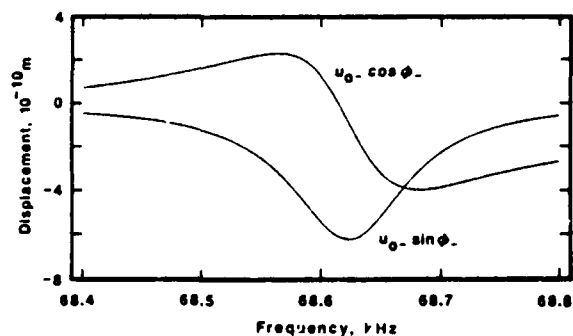


FIG. 3. Amplitudes of the in-phase, $u_{0+} \cos \phi_+$, and quadrature, $u_{0-} \sin \phi_-$, components of the (0,2) mode at the center of the — surface versus frequency. Amplitude of the driving voltage is 2.5 V.

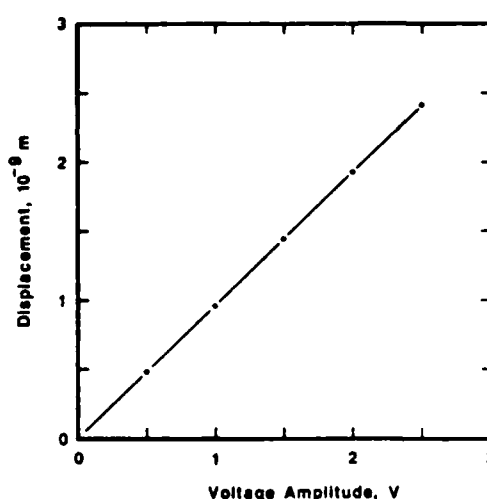


FIG. 4. Amplitude of the quadrature component, $u_{0-} \sin \phi_-$, of the (0,1) mode at the center of the — surface versus amplitude of the driving voltage.

III. DISCUSSION

Spurious resonances in hydrophones and microphones are not uncommon. For the case where these sensors are exposed to only acoustical excitation, they may be easily controlled to some extent by good design. However, in the case of strong mechanical excitation, such as flow turbulence, these spurious resonances can substantially increase sensor noise. An understanding of the cause of these spurious resonances would help in designing lower noise sensors. In the case of the electrically excited flexural mechanical resonances, near surface polarization does not explain the observed phenomena. Some of the observed symmetric modes could be excited by surface polarization, but the asymmetric ones could not. In addition, larger mode amplitudes were observed on some specimens after being poled; if surface polarization were the cause, then they should have been smaller. Chen⁹ has examined the constitutive equations of piezoelectricity and believes the resonances can be explained by inclusion of an induced body couple term and the subsequent choice of representation of this term. The classical terms of piezoelectricity are preserved in more general representations of the resulting constitutive relations of

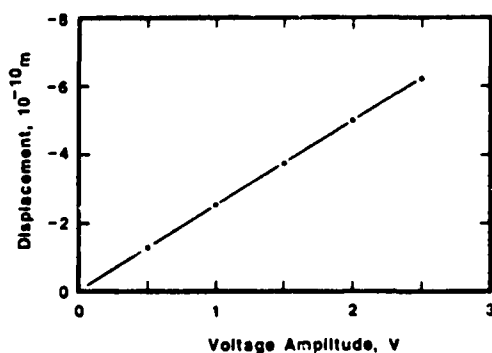


FIG. 5. Amplitude of the quadrature component, $u_{0-} \sin \phi_-$, of the (0,2) mode at the center of the — surface versus amplitude of the driving voltage.

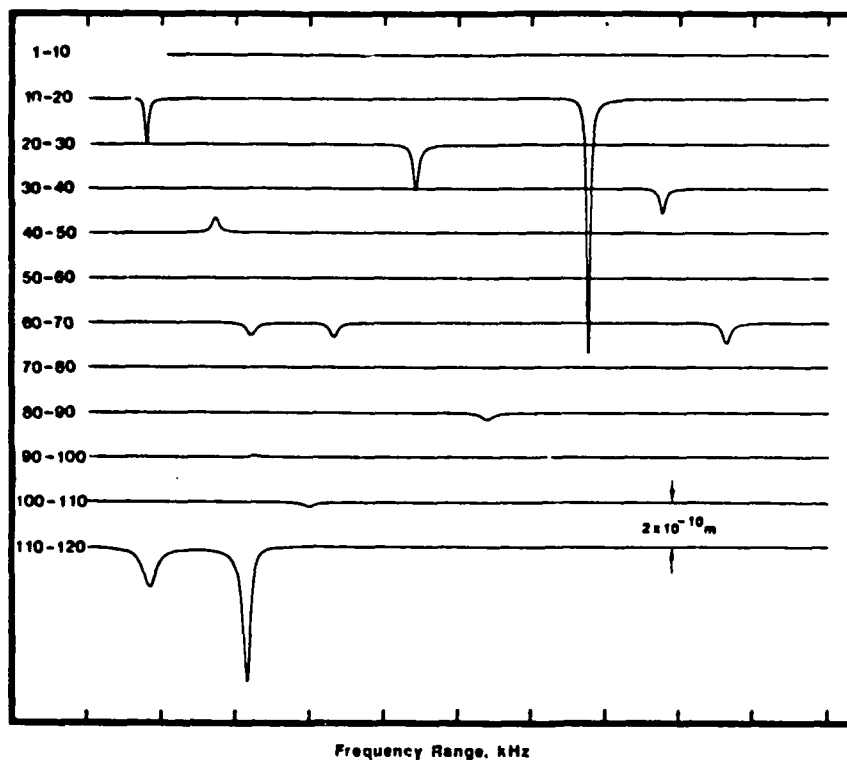


FIG. 6. Amplitude of the quadrature component, $u_0 \sin \phi_+$, at the radial location 1.119×10^{-2} m and the angular location 0° of the + surface versus frequency. Amplitude of the driving voltage is 2.5 V.

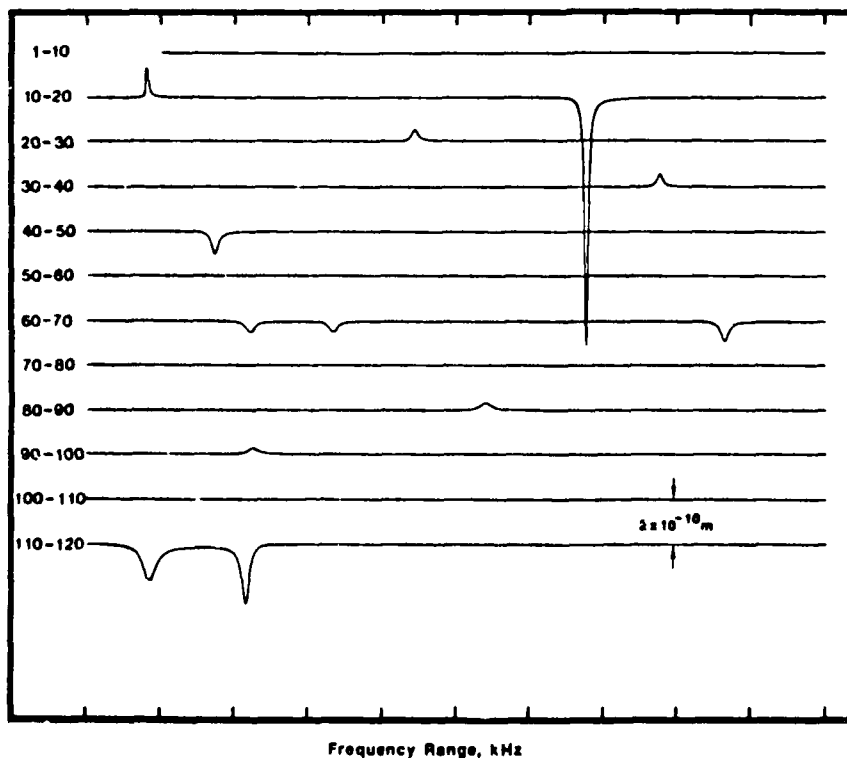


FIG. 7. Amplitude of the quadrature component, $u_0 \sin \phi_+$, at the radial location 1.119×10^{-2} m and the angular location 143° of the + surface versus frequency. Amplitude of the driving voltage is 2.5 V.

TABLE I. Ten resonances detected in the 1- to 120-kHz frequency range (see Figs. 6 and 7).

| Resonance mode | Frequency, kHz |
|----------------|----------------|
| (2,0) | 10.8 |
| (3,0) | 24.4 |
| (1,1) | 37.75 |
| (4,0) | 41.75 |
| (5,0) | 62.2 |
| (2,1) | 63.3 |
| (6,0) | 85.4 |
| (3,1) | 92.3 |
| (1,2) | 103.0 |
| (7,0) | 110.8 |

Chen's development. When we attempt to use acoustic sensors in strong flow fields, we may find that the fluid particle velocities associated with turbulent flow place us in a regime where we can no longer use the linearized equations of piezoelectricity, even though the acoustic particle velocities we may be encountering in the absence of flow would allow us to use the linear theory. More theoretical and experimental work is necessary to settle these issues.

ACKNOWLEDGMENTS

We wish to thank Dwight L. Allensworth for his expert assistance in the performance of the experiments. The work of Blue, Henriquez, and Ting was supported by the Basic

Research Program of NRL RR011-08-42. The work of Chen was performed at Sandia National Laboratories and was supported by the U. S. Department of Energy under contract number DE-AC04-76DP00789.

- ¹P. J. Chen, "Observation of the Existence of Electrically Excited Purely Mechanical Resonance in Piezoelectric and Ferroelectric Materials," *Il Nuovo Cimento* **2D**, 1145-1155 (1983).
- ²P. J. Chen, "Electrically Excitable Purely Mechanical Resonances in Piezoelectric and Ferroelectric Materials—Geometrical Considerations," *Wave Motion* **5**, 177-183 (1983).
- ³P. J. Chen, "Electrically Excitable Mechanical Resonant Mode Shapes in the Electro-optic Ceramic PLZT7/65/35," *Int. J. Solids Struct.* **22**, 909-917 (1986).
- ⁴P. J. Chen, "Certain Characteristics of Electrically Excitable Mechanical Resonant Modes of a Virgin PZT65/35 Disc," *Int. J. Eng. Sci.* **24**, 1811-1818 (1986).
- ⁵P. J. Chen, "A New Electromechanical-coupling Phenomenon in the Electro-optic Ceramic PLZT7/65/35," *Il Nuovo Cimento* **4D**, 280-292 (1984).
- ⁶P. J. Chen, "On the Nature of the Mechanical Resonance Associated with the Electrical Resonance of a Poled PZT65/35 Disc," *Wave Motion* **8**, 561-570 (1986).
- ⁷The classical bending theory of thin elastic plates does not yield solutions that exhibit phase shifts on the displacements. Mechanically dissipative theories are needed in this regard.
- ⁸A theory of electromechanical interaction based on a new concept of macroscopic body couple has been formulated recently.
- ⁹P. J. Chen, "Electrically and Mechanically Induced Macroscopic Body Couple—A Newly Recognized Phenomenon of Electromechanical Interaction," *Il Nuovo Cimento* **8D**, 481-496 (1986).
- ¹⁰R. C. Cowell and H. C. Hardy, "The Frequencies and Nodal Systems of Circular Plates," *Philos. Mag.* **S7** **24**, 1041-1055 (1937).